

Table IV. Thermal and Derived Positional Parameters of Group Atoms (All Quantities $\times 10^4$)

atom	<i>x</i>	<i>y</i>	<i>z</i>	<i>U</i> , Å ²
C(1) 1	2665 (3)	1604 (3)	5279 (2)	489 (39)
C(2) 1	2406 (3)	1790 (3)	5585 (2)	557 (43)
C(3) 1	2347 (3)	1667 (3)	6090 (2)	768 (49)
C(4) 1	2546 (3)	1357 (3)	6288 (2)	734 (51)
C(5) 1	2805 (3)	1171 (3)	5981 (2)	717 (48)
C(6) 1	2865 (3)	1294 (3)	5477 (2)	555 (42)
C(1) 2	2008 (3)	1324 (4)	4464 (3)	512 (40)
C(2) 2	1699 (3)	1526 (4)	4268 (3)	642 (46)
C(3) 2	1160 (3)	1184 (4)	4171 (3)	858 (54)
C(4) 2	931 (3)	641 (4)	4270 (3)	904 (60)
C(5) 2	1239 (3)	440 (4)	4466 (3)	783 (51)
C(6) 2	1778 (3)	782 (4)	4563 (3)	659 (46)
C(1) 3	3054 (4)	2424 (4)	3292 (3)	436 (37)
C(2) 3	2522 (4)	2024 (4)	3255 (3)	578 (44)
C(3) 3	2147 (4)	2137 (4)	3054 (3)	754 (50)
C(4) 3	2303 (4)	2651 (4)	2890 (3)	753 (49)
C(5) 3	2835 (4)	3051 (4)	2926 (3)	727 (50)
C(6) 3	3210 (4)	2938 (4)	3127 (3)	749 (49)
C(1) 4	3833 (4)	2172 (4)	2962 (3)	428 (37)
C(2) 4	4370 (4)	2479 (4)	2836 (3)	626 (45)
C(3) 4	4556 (4)	2377 (4)	2396 (3)	708 (48)
C(4) 4	4206 (4)	1968 (4)	2083 (3)	748 (51)
C(5) 4	3670 (4)	1661 (4)	2210 (3)	692 (50)
C(6) 4	3483 (4)	1763 (4)	2649 (3)	599 (42)
C(1) 5	4726 (3)	2290 (4)	4325 (3)	427 (37)
C(2) 5	4779 (3)	2161 (4)	3838 (3)	509 (40)
C(3) 5	5284 (3)	2365 (4)	3630 (3)	714 (46)
C(4) 5	5736 (3)	2699 (4)	3908 (3)	748 (54)
C(5) 5	5682 (3)	2828 (4)	4395 (3)	863 (48)
C(6) 5	5177 (3)	2624 (4)	4603 (3)	787 (50)
C(1) 6	4123 (3)	1472 (3)	5003 (3)	425 (37)
C(2) 6	4067 (3)	1446 (3)	5517 (3)	616 (45)
C(3) 6	4128 (3)	1069 (3)	5786 (3)	675 (46)
C(4) 6	4246 (3)	718 (3)	5539 (3)	652 (46)
C(5) 6	4302 (3)	743 (3)	5024 (3)	658 (47)
C(6) 6	4241 (3)	1121 (3)	4756 (3)	542 (42)

Table V. Distances (Å) and Angles (deg) in the Coordination Polyhedron with Estimated Standard Deviations in Parentheses

Distances			
Co-P(1)	2.311 (6)	Co-P(6)	2.257 (4)
Co-P(2)	2.310 (5)	P(1)-P(2)	2.137 (6)
Co-P(3)	2.325 (4)	P(1)-P(3)	2.128 (7)
Co-P(4)	2.261 (5)	P(2)-P(3)	2.139 (7)
Co-P(5)	2.243 (4)		
Angles			
P(1)-Co-P(2)	55.1 (2)	P(2)-Co-P(4)	97.4 (2)
P(1)-Co-P(3)	54.6 (2)	P(2)-Co-P(6)	97.2 (2)
P(2)-Co-P(3)	55.0 (2)	P(3)-Co-P(4)	97.1 (2)
P(1)-Co-P(4)	147.8 (1)	P(3)-Co-P(5)	97.5 (2)
P(2)-Co-P(5)	148.0 (2)	P(4)-Co-P(5)	102.6 (2)
P(3)-Co-P(6)	147.6 (2)	P(4)-Co-P(6)	103.3 (2)
P(1)-Co-P(5)	96.9 (2)	P(5)-Co-P(6)	102.1 (1)
P(1)-Co-P(6)	97.2 (2)		

metal atom plays a very important role in determining whether the central nitrogen of np_3 can be bound or not to the metal. In this respect the two complexes $[(CO)Ni(np_3)]$ (d^{10} metal, N not bound, tetrahedral) and $[(CO)Co(np_3)]^+$ (d^8 metal, N bound, TBP)¹³ are a typical significant example of the effect exerted by the configuration of the metal on the ligating properties of the np_3 ligand. In the present $[(\eta^3-P_3)Co(np_3)]$ complex, where the *cyclo*-triphosphorus group donates three electrons to the d^9 cobalt atom, only three electron pairs from the donor atoms of np_3 are required by the central atom to reach the 18-outer-electron configuration. The large Co-N distance is thus attributed to the repulsion between the electron lone pair of the nitrogen atom and the 18-electron complete shell of the metal.

Acknowledgment. Thanks are expressed to Mr. F. Nuzzi and Mr. G. Vignozzi for microanalyses.

Registry No. $[(\eta^3-P_3)Co(np_3)] \cdot 0.5C_4H_8O$, 67523-78-8; $Co(BF_4)_2$, 26490-63-1.

Supplementary Material Available: A listing of calculated and observed structure factor amplitudes (22 pages). Ordering information is given on any current masthead page.

References and Notes

- M. Di Vaira, C. A. Ghilardi, S. Midollini, and L. Sacconi, *J. Am. Chem. Soc.*, **100**, 2550 (1978).
- R. Morassi and L. Sacconi, *Inorg. Synth.*, **16**, 174 (1976).
- L. Sacconi, I. Bertini, and F. Mani, *Inorg. Chem.*, **7**, 1417 (1968).
- P. W. R. Corfield, R. J. Doedens, and J. A. Ibers, *Inorg. Chem.*, **6**, 197 (1967).
- The absorption correction program AGNOST, other computer programs such as ORTEP for molecular drawings, and the main routines of Xray-72 system for data reduction and Fourier syntheses were obtained from different sources and locally implemented on a CII 10070 computer.
- D. T. Cromer and J. T. Waber, *Acta Crystallogr.*, **18**, 104 (1965).
- R. F. Stewart, E. R. Davidson, and W. T. Simpson, *J. Chem. Phys.*, **42**, 3175 (1965).
- J. M. Stewart, F. A. Kundall, and J. C. Baldwin, Ed., "X-Ray 72", Technical Report TR 192, University of Maryland, 1972.
- C. Mealli, P. L. Orioli, and L. Sacconi, *J. Chem. Soc. A*, 2691 (1971); P. Dapporto, L. Sacconi, *ibid.*, 1804 (1970).
- L. R. Maxwell, S. B. Hendricks, and V. M. Mosley, *J. Chem. Phys.*, **3**, 699 (1935).
- A. S. Foust, M. S. Foster, and L. F. Dahl, *J. Am. Chem. Soc.*, **91**, 5631 (1969).
- Chem. Soc., Spec. Publ.*, No. 11 (1958).
- C. A. Ghilardi, A. Sabatini, and L. Sacconi, *Inorg. Chem.*, **15**, 2763 (1976).

Contribution from Oak Ridge National Laboratory,
Oak Ridge, Tennessee 37830

Refinement of the Crystal Structure of Orthorhombic Zinc Chloride¹

H. L. Yakel*² and J. Brynestad³

Received March 20, 1978

The preparation and an approximate crystal structure of an orthorhombic form of anhydrous zinc chloride were reported recently.⁴ Transitions of this form to one or more of the modifications described by Brehler⁵ were noted experimentally when the material was examined under conditions that excluded air in a less than stringent manner. A refinement of the approximate structure of orthorhombic zinc chloride has been carried out, and the results are summarized in this note.

Experimental Section

A single crystal with dimensions roughly 0.1 mm \times 0.1 mm \times 0.04 mm was isolated from crushed fragments of orthorhombic zinc chloride that had been melted and recrystallized in a temperature gradient according to the Stockbarger method.⁴ All operations with this material were performed in a helium-filled drybox with <2 ppm of H_2O and <6 ppm of O_2 . The selected crystal was forced into a tapered section of a cleaned, thin-walled glass capillary that was then fused shut with a Pt hot wire. After preliminary X-ray diffraction photographs disclosed reasonable mosaic spread and orientation, the crystal was transferred to an automated Picker diffractometer for collection of intensity data using Nb-filtered $Mo K\alpha$ X radiation (λ 0.7107 Å).

Measurements of Bragg angles of six representative reflections showed no significant differences from those predicted with the reported unit cell parameters at 20 ± 1 °C, viz., $a = 6.443$ (2) Å, $b = 7.693$ (4) Å, and $c = 6.125$ (4) Å.⁴ Intensities of 688 reflections in what was assumed to be the $+h, +k, +l$ octant of reciprocal space were recorded in an ω -scan mode. The assumption is required in view of the proposed polar space group $Pna2_1$. Since typical rocking curves for this crystal were 0.5 to 1.0° in breadth, each reflection was scanned over a 3° ω range at 0.05° steps, with a 5-s counting time at each step. Data were collected to 60° 2θ at which angle diffracted intensities had fallen to background levels for the counting parameters used.

Table I. Positional and Thermal Parameters (Multiplied by 10^4) with Estimated Standard Deviations in Parentheses

atom	x	y	z	β_{11}	β_{22}	β_{33}	β_{12}	β_{13}	β_{23}
Zn	818 (3)	1251 (2)	3750 ^a	116 (3)	86 (3)	136 (4)	-13 (3)	5 (12)	15 (11)
Cl(1)	702 (6)	1223 (11)	41 (5)	209 (9)	110 (6)	77 (7)	-18 (16)	-4 (13)	-20 (15)
Cl(2)	841 (6)	6332 (11)	-62 (6)	107 (6)	96 (6)	195 (8)	-4 (14)	7 (14)	30 (16)

^a Arbitrarily chosen z parameter permitted by the polar space group $Pna2_1$.

Background ω scans for reflections in the 20–60° 2θ range were performed with 1.6° 2θ offsets; in an overlapping 5–30° 2θ range, 1.0° 2θ offsets were chosen. Regularly repeated measurements of a strong standard reflection (040) indicated a standard deviation of 0.03, but replicate measurements of reflections in the 20–30° 2θ overlap zone suggested a higher overall standard deviation of 0.08.

Observed data were reduced to relative observed F^2 values by standard procedures. An explicit absorption correction was introduced via the ORABS-2 calculation⁶ using measured crystal dimensions and atomic mass absorption coefficients taken from standard sources.⁷ Variances in the observations were computed as the counting statistics augmented by a fractional systematic error of 0.05. Of 481 independent measured reflections allowed by the $Pna2_1$ space group,⁴ only 272 had F^2 values greater than the net anticipated error, $\sigma(F^2)$ —a condition caused by atomic positional parameters related so as to produce many accidentally weak or absent reflections.

Initial atom positions for the refinement were assumed to be those of the reported approximate structure.⁴ Rough values of a scale and an overall temperature factor were estimated from measured and calculated values of $|F|$ for the 040 and 080 reflections to which all atoms contribute approximately in phase. Atomic scattering factors and anomalous dispersion corrections were taken from standard sources.^{8,9} The structure refinement procedure selected was a least-squares analysis that minimized squares of residuals of F_i^2 weighted according to $1/\sigma_i^2$. An attempted refinement of the initial model, which used all observations with no constraints, failed, apparently because of nonlinearities arising from non space group relationships among some atom positions of the model. The situation was remedied by applying slack constraints¹⁰ to damp changes in ill-conditioned variables and to fix the tetrahedral coordination of chloride ions about zinc. These constraints were removed in the final stages of refinement that incorporated all data.

Convergence was obtained in seven least-squares cycles; atomic coordinates and anisotropic thermal vibration parameters from the last are given in Table I. Usual indices of agreement, as defined, for example, by Brown and Chidambaram,¹¹ were computed to be $R(F^2) = 0.087$ (all reflections), $R(F^2) = 0.079$ (all reflections with $F_i^2 > \sigma_i$), $\sigma_1 = 0.59$ (all reflections), and $\sigma_1 = 0.76$ (all reflections with $F_i^2 > \sigma_i$). The fact that σ_1 values are significantly less than unity probably reflects inappropriate weighting of the data set. Since the structure of orthorhombic zinc chloride is polar in the c direction, the observed data might have been collected in an octant of reciprocal space in which l was negative. This hypothesis could be tested because of the relatively large value of $\Delta f''$ for zinc with Mo $K\alpha$ radiation.⁹ Least-squares refinements using negative reflection indices gave a result that enabled the hypothesis to be rejected at a 0.99 confidence level ($R_w(+l) = 0.092$, $R_w(-l) = 0.100$).¹²

Discussion

As previously reported,⁴ the crystal structure of orthorhombic zinc chloride approximates a hexagonal sequence of close-packed chloride ion layers lying normal to c in which zinc ions occupy certain tetrahedral holes. Atom positions in the refined structure differ from those of the approximate model by at most 0.1 Å. Important interatomic distances and angles computed from the coordinates of Table I are listed in Table II. The tetrahedral environment of chloride ions about zinc is relatively regular; the small differences among Zn–Cl distances are barely significant, and departures from the ideal tetrahedral angle are limited to +2 and -1°. The average Zn–Cl distance corresponds to the shortest of those reported by Brehler⁵ and is about equal to the sum of tetrahedral covalent radii for the atoms.¹³ The Cl–Cl distances within $ZnCl_4$ tetrahedra approach the minimum expected for an ionic radius of 1.81 Å,¹³ while those between tetrahedra are several tenths of 1 Å longer.

Table II. Selected Bond Distances (Å) and Angles (deg) with Estimated Standard Deviations in Parentheses

Intratetrahedral Distances about Zn			
Zn–Cl(2,2,565) ^a	2.265 (7)	Zn–Cl(2,3,545)	2.273 (4)
Zn–Cl(1,1,555)	2.273 (4)	Zn–Cl(1,2,555)	2.282 (8)
Intratetrahedral Cl–Cl Distances			
Cl(1,1,555)–Cl(2,2,565)	3.677 (8)	Cl(1,1,555)–Cl(1,2,555) ^b	3.707 (9)
Cl(2,1,555)–Cl(2,4,565) ^c	3.689 (8)	Cl(1,1,555)–Cl(2,3,545)	3.737 (5)
Cl(1,1,555)–Cl(2,4,455)	3.698 (8)	Cl(1,1,555)–Cl(2,1,545)	3.76 (1)
Intratetrahedral Angles about Zn			
Cl(2,2,565)–Zn–Cl(1,1,555)	108.3 (2)	Cl(1,1,555)–Zn–Cl(2,3,545)	110.6 (1)
Cl(2,2,565)–Zn–Cl(2,3,545)	108.8 (2)	Cl(1,1,555)–Zn–Cl(1,2,555)	108.9 (2)
Cl(2,2,565)–Zn–Cl(1,2,555)	111.8 (2)	Cl(2,3,545)–Zn–Cl(1,2,555)	108.6 (2)
Intertetrahedral Cl–Cl Distances			
Cl(1,1,555)–Cl(1,4,555) ^b	3.773 (9)	Cl(2,1,555)–Cl(2,2,565) ^c	3.841 (9)
Cl(1,1,555)–Cl(2,2,564)	3.781 (8)	Cl(1,1,555)–Cl(2,4,555)	3.852 (8)
Cl(1,1,555)–Cl(2,3,544)	3.839 (5)	Cl(1,1,555)–Cl(2,1,555)	3.93 (1)

^a The zinc ion is the one whose coordinates are defined in Table I. Chlorine ions are designated by three integers. The first corresponds to the identification of crystallographically distinct chlorine ions defined in Table I. The second corresponds to one of the four symmetry-related positions of space group $Pna2_1$ in the order in which they appear in ref 14. The third integer is a unit cell translation indicator that follows the pattern established by Johnson.¹⁵ ^{b,c} Two symmetry-equivalent distances exist in the nearest-neighbor coordination of (b) Cl(1,1,555) and (c) Cl(2,1,555), respectively.

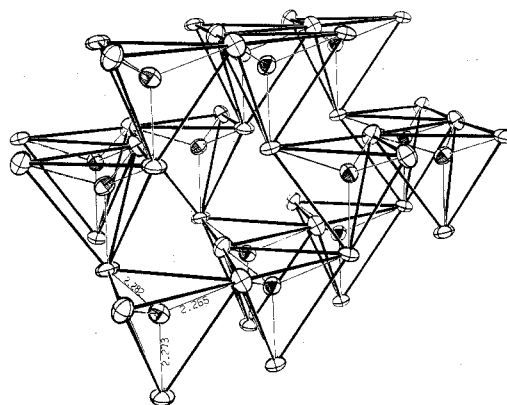


Figure 1. A portion of the crystal structure of orthorhombic zinc chloride. The c axis is approximately vertical and the b axis extends from left to right and emerges from the page at a 20° angle. Atoms are represented by thermal vibration ellipsoids including 50% probability. Three Zn–Cl distances in one tetrahedron are labeled to facilitate identification with atoms listed in Tables I and II.

A portion of the structure containing $ZnCl_4$ tetrahedra within four hexagonally stacked chloride ion layers is shown in Figure 1. Thermal vibration ellipsoids reflect root-mean-square displacements entirely in keeping with the distributions of near-neighbor contacts. All chloride ions are

common to two corner-sharing ZnCl_4 tetrahedra — there are no shared edges or faces. Each chloride ion thus has two zinc, six intratetrahedral chloride, and six intertetrahedral chloride ion nearest neighbors. Cl(1) ions join tetrahedra lying at adjacent levels along the c axis, while Cl(2) ions join tetrahedra lying at a given level. Zigzag chains of corner-sharing tetrahedra, internally related by a glide planes, extend parallel to the a direction at a given level. They do not share any corners with parallel chains at that level, but, utilizing 2_1 screw axes, share corners with tetrahedra at the levels above and below.

Registry No. ZnCl_2 , 7646-85-7.

Supplementary Material Available: A listing of observed and calculated F^2 values (4 pages). Ordering information is given on any current masthead page.

References and Notes

- (1) Research sponsored by the Division of Basic Energy Sciences, U.S. Department of Energy under Contract W-7405-eng-26 with the Union Carbide Corp.
- (2) Metals and Ceramics Division.
- (3) Chemistry Division.
- (4) J. Brynestad and H. L. Yakel, *Inorg. Chem.*, **17**, 1376 (1978).
- (5) B. Brehler, *Z. Kristallogr., Kristallgeom., Kristallphys., Kristallchem.*, **115**, 373 (1961).
- (6) D. J. Wehe, W. R. Busing, and H. A. Levy, "ORABS—A Fortran Program for Calculating Single Crystal Absorption Corrections", Report ORNL-TM-229, Oak Ridge National Laboratory, Oak Ridge, Tenn., 1962.
- (7) "International Tables for X-Ray Crystallography", Vol. III, Kynoch Press, Birmingham England, 1962, pp 162–165.
- (8) D. T. Cromer and J. T. Weber, "Scattering Factors Computed from Relativistic Dirac-Slater Wave Functions", Report LA-3056, Los Alamos Scientific Laboratory, Los Alamos, N.Mex., 1964.
- (9) "International Tables for X-Ray Crystallography", Vol. III, Kynoch Press, Birmingham, England, 1962, p 215.
- (10) A. D. Rae, *Acta Crystallogr., Sect. A*, **29**, 74 (1973).
- (11) G. M. Brown and R. Chidambaram, *Acta Crystallogr., Sect. B*, **25**, 676 (1969).
- (12) W. C. Hamilton, *Acta Crystallogr.*, **18**, 502 (1965).
- (13) L. Pauling, "The Nature of the Chemical Bond", 3rd ed., Cornell University Press, Ithaca, N.Y., 1960, p 246 (tetrahedral radii), p 514 (ionic radii).
- (14) "International Tables for X-Ray Crystallography", Vol. I, Kynoch Press, Birmingham, England, 1952, p 119.
- (15) C. K. Johnson, "ORTEP", Report ORNL-3974, Oak Ridge National Laboratory, Oak Ridge, Tenn., 1965.

Contribution from the Department of Chemistry,
Southampton University, Southampton, England

The Characterization of Molecular V_4O_{10} , an Analogue of P_4O_{10}

Ian R. Beattie,* J. Steven Ogden, and David D. Price

Received March 20, 1978

Mass spectrometric studies^{1,2} of the vapor species above heated vanadium pentoxide (1000–1200 K) have identified the prominent ions $\text{V}_4\text{O}_{10}^+$ and V_4O_8^+ , and although solid V_2O_5 does not vaporize congruently, it has been suggested² that the most abundant ion peak $\text{V}_4\text{O}_{10}^+$ arises from a molecular species V_4O_{10} isostructural with P_4O_{10} . We have carried out matrix isolation studies on this system in an attempt to characterize this interesting molecule more completely.

In a series of exploratory studies, samples of commercially available V_2O_5 (BDH) were first degassed in vacuo at $\sim 750^\circ\text{C}$ in either silica or alumina sample holders. The temperature was then raised to $800\text{--}850^\circ\text{C}$ and the vapor codeposited with an excess of nitrogen onto a CsI window cooled to $\sim 10\text{ K}$. Details of the apparatus have been described elsewhere.³ The resulting IR spectrum showed two prominent bands at 1029.9 and 828.4 cm^{-1} which always maintained the same intensity

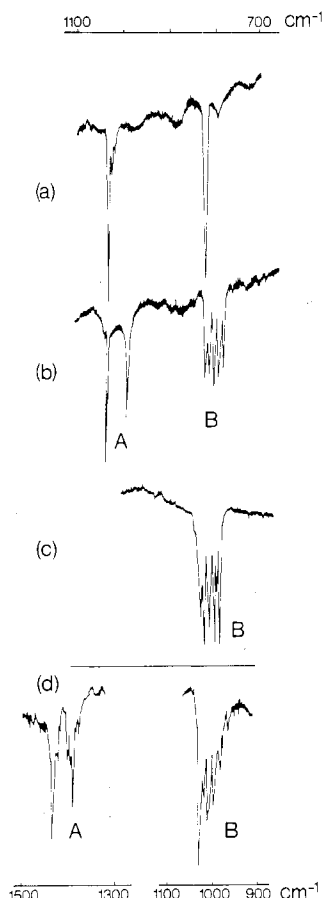


Figure 1. Matrix isolation IR absorption spectra of (a) V_4O_{10} , (b) ^{18}O -enriched V_4O_{10} , (c) ^{18}O -enriched As_4O_6 , and (d) ^{18}O -enriched P_4O_{10} .

ratio, and extended deposition yielded an additional weak feature at $\sim 626\text{ cm}^{-1}$. During deposition, a film of yellow solid was observed to condense on the cooler (off-axis) walls of the effusion chamber, and the vanadium pentoxide sample slowly turned black. The same two prominent bands were also observed from samples of substoichiometric vanadium pentoxide prepared by heating elemental vanadium in an excess of pure oxygen gas, and a typical spectrum is shown in Figure 1, part a.

The two prominent bands at 1029.9 and 828.4 cm^{-1} suggest the presence of both terminal ($\text{V}=\text{O}$) and bridge ($\text{V}-\text{O}-\text{V}$) units in the trapped species.⁴ These bands are close in frequency to two of the most prominent IR absorptions (1022 and 840 cm^{-1}) in solid vanadium pentoxide⁵ which contains both bridging and terminal oxygens. We also note that $\nu_{\text{V}=\text{O}}$ in the molecular species VOCl_3 occurs⁶ at 1035 cm^{-1} . These results, taken in conjunction with the mass spectral data and the apparent volatilization and condensation of a vanadium(V) species (yellow sublimate), indicate that molecular V_4O_{10} has been isolated in the matrix. In an attempt to confirm this, ^{18}O -enrichment studies were carried out using oxide samples prepared from vanadium metal and $^{16}/^{18}\text{O}_2$ gas.

Figure 1, part b, shows typical spectra obtained from an oxide sample enriched to the extent of $\sim 50\%$ ^{18}O . The high-frequency feature at 1029.9 now appears essentially as a prominent doublet at 1029.9 and 988.7 cm^{-1} (group A), while the 828.4-cm^{-1} band becomes an approximately equally spaced quintet at 828.4, 818.7, 809.8, 800.1, and 790.3 cm^{-1} (group B). For comparison, Figure 1, part c, shows the matrix IR spectrum⁷ of $\sim 50\%$ enriched As_4O_6 in the region of the highest T_2 cage mode ($\nu_{\text{As}-\text{O}-\text{As}}$) and Figure 1, part d, shows the matrix IR spectrum of 40% ^{18}O enriched P_4O_{10} in the